2016

1H and 19F spin-lattice relaxation and CH3 or CF3 reorientation in molecular solids containing both H and F atoms

Peter A. Beckmann
Bryn Mawr College, pbeckman@brynmawr.edu

Andrew L. Rheingold

Citation

Beckmann, P.A. and A.L. Rheingold. "1H and 19F spin-lattice relaxation and CH3 or CF3 reorientation in molecular solids containing both H and F atoms." The Journal of Chemical Physics 144, 154308 (2016); 1-12.

^{1}H and ^{19}F spin-lattice relaxation and CH_3 or CF_3 reorientation in molecular solids containing both H and F atoms

Peter A. Beckmann[1, a)] and Arnold L. Rheingold[2]

[1]Department of Physics, Bryn Mawr College, Bryn Mawr, Pennsylvania 19010-2899, USA.

[2]Department of Chemistry and Biochemistry, University of California, San Diego, 9500 Gilman Dr., La Jolla, California 92093-0358, USA.

Journal of Chemical Physics, 2016 144 154308 1-12

[a)]Author to whom correspondence should be addressed. Electronic address: pbeckman@brynmawr.edu

The dynamics of methyl (CH_3) and fluoromethyl (CF_3) groups in organic molecular (van der Waals) solids can be exploited to survey their local environments. We report solid state ^{1}H and ^{19}F spin-lattice relaxation experiments in polycrystalline 3-trifluoromethoxycinnamic acid, along with an X-ray diffraction determination of the molecular and crystal structure, to investigate the intramolecular and intermolecular interactions that determine the properties that characterize the CF_3 reorientation. The molecule is of no particular interest; it simply provides a motionless backbone (on the NMR time scale) to investigate CF_3 reorientation occurring on the NMR time scale. The effects of ^{19}F-^{19}F and ^{19}F-^{1}H spin-spin dipolar interactions on the complicated nonexponential NMR relaxation provide independent inputs into determining a model for CF_3 reorientation. As such, these experiments provide much more information than when only one spin species (usually ^{1}H) is present. In the Discussion section, which can be read immediately after the Introduction without reading the rest of the paper, we compare the barrier to CH_3 and CF_3 reorientation in seven organic solids and separate this barrier into intramolecular and intermolecular components.

I. INTRODUCTION

Methyl (CH_3) and fluoromethyl (CF_3) groups (and other similar groups) can be employed to investigate intramolecular and intermolecular interactions in their environment in a wide variety of solids.[1-25] Here we report solid state nuclear magnetic resonance (NMR) ^{1}H and ^{19}F relaxation experiments in, and an X-ray diffraction study of the molecular and crystal structure of, 3-trifluoromethoxycinnamic acid (**1**) (Fig. 1). The asymmetric unit[26] in the crystal is a single molecule, meaning that all molecules have the same environment and therefore all CF_3 groups are dynamically equivalent. In the temperature range studied, the CF_3 group is reorienting on the NMR time scale which, in the current study, we can take to mean that the mean time between CF_3 reorientations is 10^{-10} to 10^{-6} s. This is approximately two orders of magnitude on either side of

the inverse NMR frequency of 22.5 MHz. The intramolecular and intermolecular interactions that determine the reorientational CF_3 barrier are not to be confused with the spin-spin (dipolar) interactions that determine the parameters in the model used to interpret the NMR relaxation experiments. To avoid confusion, we use the terms intramolecular and intermolecular solely when discussing the former. The latter interactions have three parts: The ^{19}F spins in CF_3 groups (and they are *only* in CF_3 groups in **1**) are interacting, via spin-spin dipolar interactions, (1) among themselves in the same CF_3 group, (2) with ^{19}F spins in other CF_3 groups (on other molecules since there is only one CF_3 group per molecule), and (3) with the ^1H spins on both the same and neighboring molecules. The H atoms are not moving on the NMR time scale (the time scale for vibrations is typically 10^{-15}-10^{-14} s). In addition ^1H-^1H spin-spin energy conserving spin flips are important (in maintaining a common spin temperature[27]) even though no H-H vectors are reorienting on the NMR time scale.

We recently reported solid state ^1H and ^{19}F NMR relaxation experiments, electronic structure calculations, and X-ray diffraction experiments, to investigate CH_3 reorientation in polycrystalline 4,4'-dimethoxyoctafluorobiphenyl (**2**).[8] Half a molecule of **2**, which is the asymmetric unit in the crystal, is shown in Fig. 1 (CSD-WOQFAL[8]). The F and H atoms in **2** trade roles compared with **1**. Methoxy group (OCH_3) reorientation in **2** is quenched[8] so the CH_3 reorientation axis is not reorienting on the NMR time scale; it will undergo small-angle, high-frequency vibrations.[8] The same will be true for fluoromethoxy group (OCF_3) reorientation in **1**. We have also previously investigated CF_3 reorientation in 3-fluoromethylphenanthrene (**3**)[11, 12] (Fig. 1; CSD-QCIMOD[12]) where the CF_3 group is bonded directly to the ring. None of these compounds are of any particular interest as far as we know. Covalently bonded molecules that form van der Waals molecular solids such as **1**-**3** simply provide very stable convenient laboratories with backbone structures for CH_3 or CF_3 reorientation being the only motion on the NMR time scale, along with 'fixed' atoms (on the NMR time scale) having another spin-1/2 species, different from the spin species in the CH_3 or CF_3 rotor.

When ^1H and ^{19}F spins interact with one another, the bulk nuclear magnetization associated with either spin species, when perturbed, relaxes to its equilibrium value via a double exponential.[11, 25, 27] *Independently and in addition*, the nuclear spin-lattice relaxation of an ensemble of *isolated* CH_3 or CF_3 groups is inherently nonexponential.[28-30] Modeling the nonexponential relaxation in closed form and/or numerically due to *both* the crosstalk between ^1H

and ^{19}F spins *and* due to the inherent nonexponential relaxation of the three-spin ½ system would be unwieldy. Fortunately, it is not necessary to consider both phenomenon simultaneously. One occurs predominantly at high temperatures[28, 29] and the other occurs predominantly at low temperatures.[8, 11] In Sec. II we discuss the experimental procedure needed to characterize the nonexponential ^{1}H and ^{19}F spin-lattice relaxation. In Sec. III, we set up the model that presents the parameters used to interpret the observed spin-lattice relaxation. We seek the simplest model that fits the data in the sense that it reproduces the general (and somewhat complicated) features of the temperature dependence of both the ^{1}H and ^{19}F relaxation rates. This involves five adjustable parameters and they are all defined rigorously in Sec. III. (1) There is an NMR activation energy closely related to a barrier to CF_3 (or CH_3) reorientation.[31-35] In the Conclusions (Sec. IV) we divide this into an intramolecular and an intermolecular component and compare the two components in seven compounds similar to **1**-**3** (**1**-**3** and four others). Covalent bonds keep the molecule together as a unit, even in the solid, so, it is convenient to *define* the intramolecular interactions as those present in an isolated molecule. Then the intermolecular interactions are *defined* as the difference between the total interactions in the solid *minus* the isolated molecule interactions. This is an approximation because in the solid state the intramolecular interactions will be different from what they are in the isolated molecule because the structure of the molecule in the solid will be different from the structure of the molecule when it is isolated. But its a helpful approach. (2) There is a preexponential factor in an Arrhenius relationship but NMR relaxation experiments don't determine this parameter very accurately. (3) There is a phenomenological dimensionless parameter that is a measure of the strength of the interactions between ^{1}H and ^{19}F spins.[8, 11] Although the ^{19}F component of the spin-lattice relaxation is dominated by the modulation of the intraCF_3 ^{19}F-^{19}F spin-spin interactions (the strength of which involves *no adjustable parameters*) by CF_3 reorientation, there is (4) another phenomenological dimensionless parameter that is a measure of the interactions between ^{19}F spins on different CF_3 groups, assuming all F atoms are found in CF_3 groups as in **1** and **3**[11] (or between ^{1}H spins on different CH_3 groups assuming all H atoms are found in CH_3 groups as in **2**[8]). (5) Finally, there is a parameter that characterizes a (very small) distribution of NMR activation energies for CF_3 reorientation. We restrict ourselves to the case where all atoms with one spin-1/2 nuclear spin species are in a group (CH_3 or CF_3) reorienting on the NMR time scale and all the other spin-1/2 nuclear spin species are not moving on the NMR time scale as in **1**-**3** in Fig. 1.

Readers not interested in the details of the NMR relaxation experiments or the X-ray diffraction experiments are invited to go directly to the Discussion section (Sec. IV) which provides a discussion of the barriers to CF_3 and CH_3 reorientation in seven organic solids, including **1**, **2**, and **3**. Finally, as an aside, we note for completeness that because the reorientational properties of methyl groups in the solid state provide information concerning their environment, spin-lattice relaxation experiments are becoming very helpful in investigating the intramolecular and intermolecular interactions in biologically relevant molecules.[36-55]

II. THE EXPERIMENTS

A. X-ray diffraction.

The sample of 3-trifluoromethoxycinnamic acid (**1**) was purchased from Sigma Aldrich and used as is. The quoted purity was 97%. A single crystal, taken from the same polycrystalline sample used to perform the solid state NMR relaxation experiments, was mounted on a Hampton CryoLoop with Paratone-N and data collected with a Bruker D8 diffractometer using an Ultra rotating-anode generator (Mo) equipped with a high-efficiency multilayer, double-bounce monochromator. Experimental details are collected in Table I. All data were collected with 1.0 sec/1.0^{O} correlated scans. Structure solution and subsequent refinement used various components of the SHELXTL software package distributed by the Bruker Corporation (G. Sheldrick, Bruker-AXS, Madison WI). The molecular structure (in the crystal) is shown in Fig. 1 and the crystal structure is shown in Fig. 2.

B. Solid state NMR relaxation.

Solid state ^{1}H and ^{19}F spin-lattice relaxation was observed between 120 and 320 K at an NMR frequency of $\omega/2\pi$ = 22.50 MHz using a (perturbation π)-t-(observe $\pi/2$)-t_w pulse sequence. The wait time t_w was sufficiently long to allow the magnetization to return to its equilibrium value within 0.1 %. Unlike most high frequency NMR *spectroscopy* experiments involving different spin species, which are done at constant magnetic field, the *relaxation* experiments reported here are performed at constant NMR frequency. The magnetic field was 0.5285 T when ^{1}H nuclei were observed and 0.5617 T when ^{19}F nuclei were observed. Another difference is that the NMR frequency (22.5 MHz) being used here is very low compared with conventional high resolution NMR spectroscopy experiments. This is needed in order to bring the frequencies for CF_3 group

reorientation into resonance with the NMR frequency in a temperature range below the melting points of solids like **1**, **2**, and **3**.

The various parameters that characterize the relaxation are presented as a function of temperature in Figs. 3 and 4. Temperature was controlled with a flow of cold nitrogen gas and temperature was measured with a home-made, silver-soldered, copper-constantan thermocouple imbedded in a part of the sample just outside the NMR coil. Absolute temperature was measured to ± 2 K and temperature differences were monitored to ± 0.3 K. The thermocouples used in the laboratory are calibrated to four secondary temperature standards and the calibration is checked every few years.

Exponential relaxation is characterized by

$$M(t) = M(\infty)\left[1-(1-\cos\theta)\exp(-Rt)\right]. \qquad (1)$$

R is the spin-lattice relaxation rate (the inverse of the spin-lattice relaxation time T_1) and $M(\infty)$ is the equilibrium magnetization. The parameter θ characterizes the perturbation pulse since $M(0) = [\cos\theta]M(\infty)$. Ideally $\theta = \pi$ in the present case but in fact θ can differ from π just enough to produce systematic errors in the other parameters if it, itself, is not taken as an adjustable parameter. There are three adjustable parameters, R, $M(\infty)$, and θ [or $M(0)$]. *The relaxation reported here was never exponential and never described by Eq.1.*

The relaxation was nonexponential at all temperatures for both ^{1}H and ^{19}F. Above 172 K (region I in Figs. 3 and 4) the recovering perturbed magnetization (^{1}H or ^{19}F) was well fitted to a four-parameter stretched exponential:[56-66]

$$M_{\mathrm{k}}(t) = M_{\mathrm{k}}(\infty)\left[1-(1-\cos\theta)\exp\left\{-\left(R_{\mathrm{k}}^{*}t\right)^{\beta}\right\}\right], \qquad (2)$$

for k = H or F. The characteristic relaxation rate R_{k}^{*} in Eq. 2 replaces the relaxation rate R in Eq. 1, and Eq. 2 introduces a fourth parameter β, the stretching parameter. (Whereas R_{F}^{*} and R_{H}^{*} differ greatly, β is relatively insensitive to which spin species is being investigated.) In an NMR relaxation experiment, the parameters R_{k}^{*} and β are not amendable to interpretation by any closed-

form model as far as we are aware. However, $\beta < 1$ is a quantitative measure of the nonexponentiality of the relaxation and measuring it is important because it imposes conditions on performing the relaxation measurements. Care must be taken when performing nonexponential relaxation experiments because the recovery at long times is 'stretched' and $M(\infty)$ must be accurately established. In order to ensure that the relaxed magnetization is within 0.1 % of its 'true' equilibrium value, the wait time t_w is $t_w > (7R^*)^{1/\beta}$ and we generally ensure that the value is $t_w > (8R^*)^{1/\beta}$. The parameter β versus T^{-1} above 172 K (region I) is shown in Fig. 4.

For this same temperature range (region I in Figs. 3 and 4), the initial relaxation rate R_S characterizing the short-time recovery,

$$(R_k)_S = -\left(\frac{\left[\frac{d\{M_k(\infty) - M_k(t)\}}{dt}\right]}{M_k(\infty) - M_k(t)}\right)_{\lim t \to 0}, \qquad (3)$$

for k = H or F, was determined since this is the parameter that can be modeled (Sec. III) when the relaxation is well characterized by the stretched exponential in Eq. 2. The procedure for determining $(R_k)_S$ in practice is outlined in detail elsewhere.[6]

At temperatures below 160 K (region III in Figs. 3 and 4) the relaxation is characterized by a five-parameter double exponential:

$$M_k(t) = M_{1k}(\infty)\left[1-(1-\cos\theta)\exp(-\lambda_1 t)\right] + M_{2k}(\infty)\left[1-(1-\cos\theta)\exp(-\lambda_2 t)\right], \qquad (4)$$

with adjustable parameters λ_1, λ_2, $M_{1k}(\infty)$, $M_{2k}(\infty)$ (k = H or F), and θ. The observed rates λ_1 and λ_2 are shown in Fig. 3 and the four observed fractional equilibrium magnetizations,

$$\phi_{jk} = \frac{M_{jk}(\infty)}{M_{1k}(\infty) + M_{2k}(\infty)}, \qquad (5)$$

with j = 1,2 and k = H or F are shown in temperature region III Fig. 4. In this region both spin species relax with the same two relaxation rates λ_1 and λ_2 and the same two equilibrium fractional magnetizations.[11] The reason for a subscript k = F or H on ϕ_{1k} and ϕ_{2k} in Eq. 4 is subtle (and necessary) and is discussed in Sec. III. The wait time t_w was always $t_w > 8\lambda_2^{-1}$ where $\lambda_2 < \lambda_1$.

When the relaxation is nonexponential, it is important to establish that a four parameter fit (Eq. 2) to the relaxing magnetization will not work before employing a five-parameter fit (Eq. 4) otherwise the fit has an unnecessary number of adjustable parameters. An example is shown in Fig. 5 where the five-parameter double exponential fits the recovery very well but the four-parameter stretched exponential is a poor fit. The "step" in the magnetization recovery curve in the vicinity of 300 ms in Fig. 5 indicates that a double exponential fit is appropriate. The time axis in Fig. 5 is presented on a logarithmic scale solely to make the data and fits more clear. Note that the time spans more than four orders of magnitude in order to appropriately characterize two relaxation rates λ_1 and λ_2 that differ by more than a factor of ten.

The region between 160 and 172 K (region II) is a segue between the two regions I and III and, in general, neither a four-parameter stretched exponential or a five-parameter double exponential fits the relaxing magnetization very well. However, in this region in Fig. 3 we show the (somewhat meaningless) values of R_k^* (closed squares) from the stretched exponential and $(R_k)_S$ (closed circles), the initial short-time relaxation rate, to indicate the significant difference between the behavior of the ^{19}F relaxation rates between regions I and III (the ^{19}F spins being the "relaxing spins") and the behavior of the ^{1}H relaxation rates (the ^{1}H spins being the "non-relaxing spins" relaxed by the ^{19}F spins). (This region II is left blank in Fig. 4.)

III. THE THEORETICAL MODEL AND AN ANALYSIS OF THE EXPERIMENTAL RESULTS

The Bloch-Wangsness-Redfield model of nuclear spin-lattice relaxation,[27, 67-75] motivated by the original Bloembergen-Purcell-Pound experiments,[67] is the basis of the somewhat complicated and multifaceted NMR spin-lattice relaxation model presented here. We first consider a system comprised of isolated and randomly, isotropically orienting, spin-1/2 pairs (^{19}F-^{19}F or ^{1}H-^{1}H but we will use ^{19}F-^{19}F as the example here since that is the case for **1**) with fixed F-F distances r_{FF}. In addition, the motions (the reorientations of the vectors $\vec{r}_{FF}$) of the isolated pairs

are uncorrelated and only autocorrelation functions are involved.[27] In this case, a perturbed ^{19}F magnetization $M(t)$ relaxes exponentially according to Eq. 1 with[27]

$$R = A\left[J(\omega,\tau) + 4J(2\omega,\tau)\right], \tag{6}$$

$$A = \frac{3}{20}\left(\frac{\mu_0}{4\pi}\right)^2\left(\frac{\hbar\gamma_F^2}{r_{FF}^3}\right)^2, \tag{7}$$

$$J(\omega,\tau) = \frac{2\tau}{1+\omega^2\tau^2}, \tag{8}$$

$$\tau = \tau_\infty e^{E_{NMR}/kT}. \tag{9}$$

Here, μ_0 is the magnetic constant, γ_F is the ^{19}F magnetogyric ratio, $J(\omega, \tau)$ is the spectral density [the angular frequency spectrum of the local time-dependent magnetic fields resulting from the motion (reorientation) of the constant length spin-spin vectors $\vec{r}_{FF}$], ω_F is the ^{19}F NMR angular frequency [= (2π)(22.5 MHz) in this work], τ is the correlation time that can be taken to be the mean resident time between reorientations in a Poisson reorientational process,[76-85] τ_∞ is a preexponential factor whose inverse can be taken as a vibrational frequency at the bottom of the well or, equivalently, a reorientation attempt frequency,[78, 86-88] and E_{NMR} is an NMR activation energy that is closely related to the barrier that a spin pair must overcome in order to reorient; that is, to reorient from one orientation to another. The Discussion section (Sec. IV) of this paper presents a discussion of E_{NMR} in seven related compounds. If we applied this model (inappropriately so) to the high-temperature linear $\ln(R_k)_S$ versus T^{-1} (k = H *and* F) relaxation rate data in Fig. 3, $E_{NMR} = 23 \pm 2$ kJ mol^{-1} and, interestingly enough, this value of E_{NMR} will not change in the subsequent required refinements of the model. It is simply the slope of $\ln(R_k)_S$ versus T^{-1}.

If we now account for the fact that there are three spins in a CF_3 group then the factor of 3/20 in Eq. 7 is multiplied by 6/3 = 2 since there are now six interactions and three spins[76, 77] as opposed to the two interactions involving two spins as presented in the previous paragraph. If, in

addition, we account for the fact that the reorientation axis is always $\alpha = 90^{O}$ from the reorienting $\vec{r}_{FF}$ vectors, there is an additional factor of[76, 77]

$$\Lambda(\alpha) = \frac{3}{4}\left(\sin^4\alpha + \sin^2 2\alpha\right) \quad , \tag{10}$$

which equals ¾ for $\alpha = 90^{O}$. Thus the relaxing ^{19}F bulk magnetization in a polycrystalline sample *would* (were it not for additional required refinements to the model presented below) be given by Eqs. 1 and 6-9 with the parameter 3/20 in Eq. 7 replaced by 9/40.[76, 77]

CF_3 group reorientation, though random, is not isotropic; the three F-F vectors $\vec{r}_{FF}$ in any given CF_3 group in the solid reorient in a plane. In addition, the motion of the three $\vec{r}_{FF}$ vectors are 100% correlated. Runnels[28] and Hilt and Hubbard[29] dealt with these complications in detail. The motion of the three spins and the fact that there are eight spin states introduces *cross*-correlation functions as well as the *auto*-correlations functions that characterize isolated spin pairs.[28, 29] If all the CF_3 group reorientation axes are oriented with the same angle with respect to the applied magnetic field (this is *not* the angle α in Eq. 10), the relaxation involves the sum of four exponentials and can be presented in closed form.[28, 29] When the reorientation axes are distributed randomly as in a polycrystalline sample, a numerical average (of the angle between the reorientation axes and the applied magnetic field) must be computed and the relaxation is still nonexponential, especially near the relaxation rate maximum ($\omega_F\tau \sim 1$) and at higher temperatures ($\omega_F\tau < 1$).[29] This has been observed in many experiments.[2, 6, 89-95] (Note that this nonexponential relaxation has nothing to do with the biexponential relaxation resulting from ^{1}H-^{19}F spin-spin interactions which we have not "turned on" yet. We are still considering only CF_3 groups isolated from one another and from all other spins.) In this case the relaxation is accurately described by the stretched exponential in Eq. 2.[89] This is simply an experimental result and has nothing to do with the model. In this case, the *initial* relaxation rate[6] R_S, defined by Eq. 3 is characterized by Eqs. 6-9.[29] We replace Eqs. 6 and 7 with

$$(R_{FF}^{L\,intra})_S = K_{FF}^{L\,intra}\left[J(\omega_F,\tau) + 4J(2\omega_F,\tau)\right], \tag{11}$$

$$K_{\mathrm{FF}}^{\mathrm{L\,intra}} = \frac{9}{40}\left(\frac{\mu_0}{4\pi}\right)^2\left(\frac{\hbar\gamma_{\mathrm{F}}^2}{r_{\mathrm{FF\,intra}}^3}\right)^2 = 9.51\times10^8\ \mathrm{s}^{-2}. \qquad (12)$$

The cumbersome notation is necessary. The superscript L on $(R_{\mathrm{FF}}^{\mathrm{L\,intra}})_{\mathrm{S}}$ and $K_{\mathrm{FF}}^{\mathrm{L\,intra}}$ reminds us that the interactions involved are among like spins (in this case ^{19}F spins) and the superscript 'intra' refers to the six intraCF_3 group ^{19}F-^{19}F spin-spin interactions. The subscript FF indicates that the (like) spin-spin interactions being considered involve ^{19}F spins. Again, the subscript S reminds us that when the relaxation is nonexponential because of the Hilt-Hubbard-Runnells effects[28, 29] then Eq. 11 refers to the initial relaxation rate defined experimentally in Eq. 3. The distance between F atoms in the CF_3 group $r_{\mathrm{FF\,intra}}$ in Eq. 12 is known from X-ray diffraction and $K_{\mathrm{FF}}^{\mathrm{L\,intra}}$ is *not* an adjustable parameter. The main reason that Eqs. 11, 3, and 12 are valid for short times following a perturbation is that the effects of cross correlations do *not* manifest themselves at short times. That is, with the adjustments to numerical factors that now appear in Eq. 12, the three pairs of spins in a CF_3 group 'appear' as independent pairs of isolated spins for $t << (R^*)^{-1}$ in Eq. 2.

For completeness we note that (now using CH_3 groups as the example), the presence of either ^{1}H spin-spin interactions between CH_3 group ^{1}H spins and other ^{1}H spins or between ^{1}H spins on different CH_3 groups makes the relaxation more exponential.[95, 96] This has been born out in experiments with solids comprised of larger organic molecules with several or many static (on the NMR time scale) H atoms. In some of these cases, the departure from exponential relaxation is very slight or not observed at all.[97-99]

We introduce the Davidson-Cole spectral density[4, 100]

$$J(\omega,\tau) = \frac{2}{\omega}\frac{\sin\left[\varepsilon\arctan(\omega\tau)\right]}{\left(1+\omega^2\tau^2\right)^{\varepsilon/2}}, \qquad (13)$$

which replaces the BPP[67] spectral density in Eq. 8. This allows for a very small distribution of correlation times (characterized by $\varepsilon < 1$) with τ being the ideal crystal NMR correlation time.[4] As $\varepsilon \rightarrow 1$, $J(\omega,\tau)$ in Eq. 13$\rightarrow J(\omega,\tau)$ in Eq. 8. The BPP[67] spectral density in Eq. 8 will not fit data if the magnitudes of the slopes of the low and high-temperature linear ln$R$ versus T^{-1} are different

(assuming that a single motion is responsible for the relaxation in the entire temperature region studied). In the Davidson-Cole spectral density, ε is the ratio of the magnitudes of these two slopes.[16] In the present case, $\varepsilon = 0.85 \pm 0.03$ and this will not change in the subsequent complications of the model. The distribution of E_{NMR} values for $\varepsilon = 0.85$ is so small[101] that without any loss of generality or consistency, E_{NMR} can be taken as 'the' single NMR activation energy.

As an example of the predictions of the model developed so far (isolated CF_3 groups), the contribution to the ^{19}F relaxation data corresponding to Eqs. 11-13, and 9 in **1** is shown by the single line labeled $q = 0$ (q is defined below) in Fig. 6. $(R_{FF}^{L\ intra})_S = \lambda_1$ in region I, the fit to which will not change significantly in further refinements to the model presented below. Note that the only additional adjustable parameter for this $\ln\lambda_1$ versus T^{-1} in region I (once E_{NMR} and ε have been determined) is τ_∞ in Eq. 9. The high temperature $(R_{FF}^{L\ intra})_S = \lambda_1$ values are fit very well as are the λ_2 component of the low-temperature rates.

The model presented above has been appropriately modified[11, 25, 27] and applied to a system with two spin-1/2 species whose NMR frequencies are close enough that mutual spin flips can occur. The energy difference involved with mutual spin flips involving different spin species, if small enough (which is the case for ^{19}F and ^{1}H spins) is made up by the heat bath (lattice vibrations). In the present case (compound **1** in Fig. 1), CF_3 reorientation occurs on the NMR time scale and the ^{19}F spins are the "prime relaxors." (All ^{19}F spins are in CF_3 groups.) The same is true for **3**.[11] The ^{1}H spins are immobile (on the NMR time scale) and are relaxed by the relaxing ^{19}F spins via mutual spin flips. In **2**,[8] the opposite is true; the F and H atoms trade places with those of **1** and **3**.

Many experiments have been reported where both ^{1}H and ^{19}F spin-lattice relaxation rates have been measured.[1, 8-9, 11, 13-14, 17-25] In general, for a system with both ^{1}H and ^{19}F spins (or any two spin-1/2 species for that matter), the time dependence of the ^{19}F and ^{1}H nuclear magnetizations following a perturbation is given by[8, 27]

$$\frac{d}{dt}\begin{pmatrix} M_H(\infty) - M_H(t) \\ M_F(\infty) - M_F(t) \end{pmatrix} = -\begin{pmatrix} R_{HH}^{L} + R_{HH}^{U} & R_{HF}^{U} \\ R_{FH}^{U} & R_{FF}^{L} + R_{FF}^{U} \end{pmatrix}\begin{pmatrix} M_H(\infty) - M_H(t) \\ M_F(\infty) - M_F(t) \end{pmatrix}. \quad (14)$$

The superscripts 'L' on the entries in the relaxation matrix in Eq. 14 mean 'like spins' and the superscripts 'U' mean 'unlike spins.' R_{HH}^{L} characterizes the relaxation resulting from the modulation of *all* the ^{1}H-^{1}H spin-spin interactions and is identically zero in **1** and **3**. R_{FF}^{L} characterizes the relaxation resulting from the modulation of *all* the ^{19}F-^{19}F spin-spin interactions and (in **1** and **3**) is

$$R_{FF}^{L} = R_{FF}^{L\,intra} + R_{FF}^{L\,inter}, \tag{15}$$

with $R_{FF}^{L\,intra}$ given by Eqs. 11 and 12. There is now no need for the subscript 'S' in Eq. 11. Nonexponential relaxation resulting from the Hubbard-Hilt-Runnells effect[28, 29] only manifests itself at high temperatures (region I in Figs. 3 and 4) and the double exponential relaxation resulting from Eq. 14 (discussed further below) manifests itself only at low temperatures (region III in Figs. 3 and 4). In Eq. 15, $R_{FF}^{L\,inter}$ characterizes the relaxation caused by the modulation of F-F vectors between ^{19}F spins on *different* CF_3 groups and is given by

$$R_{FF}^{L\,inter} = K_{FF}^{L\,inter}\left[J\left(\omega_F, \tau/2\right) + 4J\left(2\omega_F, \tau/2\right)\right], \tag{16}$$

$$K_{FF}^{L\,inter} = \frac{3}{20}\left(\frac{\mu_0}{4\pi}\right)^2 \hbar^2 \gamma_F^4 \left\langle \frac{1}{3}\sum_{\vec{r}_{FF\,inter}} \left(\frac{\Gamma\left(\delta_{FF\,inter}\right)}{r_{FF\,inter}^{6}} \right) \right\rangle$$

$$= \frac{2}{3} K_{FF}^{L\,intra} \left\langle \frac{1}{3}\sum_{\vec{r}_{FF\,inter}} \Gamma\left(\delta_{FF\,inter}\right) \left(\frac{r_{FF\,intra}^{6}}{r_{FF\,inter}^{6}} \right) \right\rangle$$

$$= y\, K_{FF}^{L\,intra}. \tag{17}$$

A numerical value for the parameter $K_{FF}^{L\,intra}$ that appears in Eq. 17 is given in Eq. 12 so this is known. The dimensionless phenomenological parameter *y* introduced in Eq. 17 can be thought of as the *ratio of* [the overall contribution to the relaxation of all the interCF_3 ^{19}F-^{19}F spin-spin

interactions] *to* [the contribution to the relaxation of the intraCF_3 ^{19}F-^{19}F spin-spin interactions].[11] Note that the correlation time in Eq. 16 is $\tau/2$ rather than τ since it involves the random reorientation of two CF_3 groups. The angle $\delta_{\mathrm{FFinter}}$ in Eq. 17 is the angle that a particular interCF_3 vector $\vec{r}_{\mathrm{FF\,inter}}$ makes with the applied magnetic field and the function $\Gamma(\delta)$ represents, somewhat symbolically, the functions (primarily various spherical harmonics) whose modulation enters the general spin-lattice relaxation problem.[27, 67-75] Accounting for these interCF_3 ^{19}F-^{19}F spin-spin interactions in a detailed manner is an extraordinarily complicated computational problem.[102, 103] Some of these interCF_3 vectors $\vec{r}_{\mathrm{FF\,inter}}$ will undergo very small angular variations $\delta_{\mathrm{FFinter}}$ as the two CF_3 groups involved reorient and as such will contribute very little to the relaxation, even though this motion is on the NMR time scale. In addition, the strength of the spin-spin interactions go as $r_{\mathrm{FF\,inter}}^{-6}$ and so fall off very rapidly with F-F separation. We note that some of the distances $r_{\mathrm{FF\,inter}}$ appear small in Fig. 2 but this is misleading. The neighboring CF_3 groups in Fig. 2 are considerably displaced in the direction perpendicular to the page. Characterizing these interCF_3 ^{19}F-^{19}F spin-spin interactions in a more complicated manner is simply not justified by the limited information provided by the relaxation rate data. The angular brackets < . . . > in Eq. 17 indicates an ensemble average over all values of $\vec{r}_{\mathrm{FF\,intra}}$.

The single adjustable parameter y hides our ignorance. For **1**, the best fit of the data provides $y = 0.15 \pm 0.05$ and the fact that it is significantly less than unity somewhat justifies hiding our ignorance. This value for y, along with E_{NMR} and ε presented above, using only Eq. 15 for the relaxation rate, gives the same single line labeled $q = 0$ in Fig. 6 as introduced above. This line ($q = 0$) for $y = 0.15$, is indistinguishable from that as produced with $y = 0$ previously, because the as-yet not-finalized value of τ_∞ in Eq. 9 is adjusted accordingly. Finally, we note that the fact that the correlation time for $R_{\mathrm{FF}}^{\mathrm{L\,inter}}$ in Eq. 16 is $\tau/2$, rather than τ for $R_{\mathrm{FF}}^{\mathrm{L\,intra}}$ in Eq. 11 has a very small effect because it does not affect E_{NMR} which is in the exponential in Eq. 9.

The parameter $R_{\mathrm{HH}}^{\mathrm{L}}$ in Eq. 14 is identically zero for **1** (and **3**). No ^{1}H-^{1}H spin-spin interactions are modulated on the NMR time scale. The remaining four entries R^{U} in the relaxation matrix in Eq. 14 characterize the ^{1}H-^{19}F spin-spin interactions and turn the relaxation function into a double exponential. They are:

$$R_{FF}^{U} = K_{FF}^{U}\left\{J\left(\omega_H - \omega_F, \tau\right) + 3J\left(\omega_F, \tau\right) + 6J\left(\omega_H + \omega_F, \tau\right)\right\}, \tag{18}$$

$$R_{HH}^{U} = K_{HH}^{U}\left\{J\left(\omega_H - \omega_F, \tau\right) + 3J\left(\omega_H, \tau\right) + 6J\left(\omega_H + \omega_F, \tau\right)\right\}, \tag{19}$$

$$R_{FH}^{U} = R_{HF}^{U} = K_{FH}^{U}\left\{-J\left(\omega_H - \omega_F, \tau\right) + 6J\left(\omega_H + \omega_F, \tau\right)\right\}. \tag{20}$$

That there are terms in R_{FH}^{U} and R_{HF}^{U} is to be expected but that there are terms in R_{FF}^{U} and R_{HH}^{U} is, perhaps, not so obvious.[27] The four K-values are equal (but only because both spin species are spin-½) and given by

$$K_{FF}^{U} = K_{HH}^{U} = K_{FH}^{U} = K_{HF}^{U} = \frac{1}{20}\left(\frac{\mu_0}{4\pi}\right)^2 \hbar^2 \gamma_F^2 \gamma_H^2 \left\langle \sum_{\vec{r}_{FH}} \left(\frac{\Gamma\left(\delta_{FH}\right)}{r_{FH}^6} \right) \right\rangle$$

$$= \frac{2}{9}\left(\frac{\gamma_H}{\gamma_F}\right)^2 \left\langle \sum_{\vec{r}_{FH}} \Gamma\left(\delta_{FH}\right) \left(\frac{r_{FF\,intra}^6}{r_{FH}^6} \right) \right\rangle K_{FF}^{L\,intra}$$

$$= q\, K_{FF}^{L\,intra}. \tag{21}$$

Eq. 21 defines the phenomenological parameter *q* as the ratio *of* [the overall contribution to the relaxation of all the ^{1}H-^{19}F spin-spin interactions] *to* [the contribution to the relaxation of the intraCF_3 ^{19}F-^{19}F spin-spin interactions].[11] In principle, it could be computed in the same manner described for the possible computation of *y* as discussed above. Again, the single parameter *q* summarizes our ignorance concerning the details of how the modulation of the H-F vectors $\vec{r}_{FH}$ affect the relaxation and a more complicated model is not warranted.

The relaxation of either a perturbed ^{1}H or ^{19}F magnetization is given by Eq. 4 with the relaxation rates λ_1 and λ_2 (the "eigenvalues" or "eigenrates") found by diagonalizing the relaxation matrix in Eq. 14:

$$\lambda_{1,2} = \frac{1}{2}\left[\left(R_{FF}^{L} + R_{FF}^{U}\right) + \left(R_{HH}^{L} + R_{HH}^{U}\right) \pm \sqrt{\left[\left(R_{FF}^{L} + R_{FF}^{U}\right) - \left(R_{HH}^{L} + R_{HH}^{U}\right)\right]^2 + 4\,R_{FH}^{U}\,R_{HF}^{U}}\right]. \quad (22)$$

The equilibrium magnetizations ϕ_{jk} in Eq. 5 (the "eigenvectors") give the fraction of the magnetization that relaxes with each of the two eigenrates via

$$\frac{M_k(\infty) - M_k(t)}{\{1-\cos\theta\}\,M_k(\infty)} = \phi_{1k}\,e^{-\lambda_1 t} + \phi_{2k}\,e^{-\lambda_2 t}, \quad (23)$$

with k = H or F and where θ is the perturbation pulse flip angle which is very close to $\theta = \pi$. The ϕ_{jk} values are given by[8]

$$\phi_{1k} = 1 - \phi_{2k} = \frac{R_{kk}^{L} + R_{kk}^{U} - \lambda_2}{\lambda_1 - \lambda_2} \quad . \quad (24)$$

for k = F, H.

The ^{1}H-^{19}F spin-spin interactions, whose modulation results in the four R^U entries in Eq. 14 turn the *single* relaxation curve indicated by $q = 0$ in Fig. 6 into *pairs* of curves for $q \neq 0$ in Fig. 6 since the relaxation is now characterized by a double exponential.

There are five adjustable parameters. The complicated λ_1 and λ_2 versus T^{-1} over determines these parameters and we feel it is most instructive to fit the linear $\ln\lambda_1$ and $\ln\lambda_2$ versus T^{-1} data above 213 K (10^{-3} $T^{-1} < 4.7$ K^{-1} in Fig. 3) and below 143 K (10^{-3} $T^{-1} > 7.0$ K^{-1}) which uniquely determines all five parameters. The λ_1 and λ_2 versus T^{-1} between 143 and 213 K is then determined. Above 213 K, $\omega_F\tau$, $\omega_H\tau$, $(\omega_H + \omega_F)\tau$, and $(\omega_H - \omega_F)\tau$ are all << 1 and $\ln\lambda_1$ and $\ln\lambda_2$ versus T^{-1} are linear with the same slope E_{NMR} but different intercepts. Fitting these two lines gives (1) $E_{NMR} = 23 \pm 2$ kJ mol^{-1} in Eq. 9. Below 143 K, $\omega_F\tau$, $\omega_H\tau$, $(\omega_H + \omega_F)\tau$, and $(\omega_H - \omega_F)\tau$ are all >> 1 and $\ln\lambda_1$ and $\ln\lambda_2$ versus T^{-1} are again linear with the same slope $-\varepsilon E_{NMR}$ but different intercepts. This gives (2) $\varepsilon = 0.85 \pm 0.03$ in Eq. 13. The four intercepts of these two linear

relationships provide four closed-form relationships among the three parameters τ_∞, y, and q and uniquely determines them all. However, the difference between the two high-temperature intercepts and the difference between the two low-temperature intercepts depend solely on q which is over determined. That both pairs of straight lines are very well fitted with (3) $q = 0.15 \pm 0.03$ in Eq. 21 indicates that the simplest model whereby the myriad of ^{1}H-^{19}F spin-spin interaction can be modeled by the single phenomenological parameter q is justified (or, is, at least, reasonable). This leaves two (not three) closed form relationships between τ_∞ and y which give (4) $\tau_\infty = (2.2\ ^{+2.2}_{-1.1})$ X 10^{-15} s in Eq. 9 and (5) $y = 0.15 \pm 0.05$ in Eq. 17.

Although the now completely predicted λ_1 and λ_2 versus T^{-1} between 143 and 213 K reproduces the general features in the observed relaxation rates (Fig. 3), there are discrepancies which would no doubt be rectified with more robust models with a greater number of adjustable parameters. The fit for λ_1 versus T^{-1} between the two limiting regions shows two maxima, one at 190 K where $\omega_F\tau$, $\omega_H\tau$, and $(\omega_H + \omega_F)\tau \sim 1$ and one at 155 K where $(\omega_H - \omega_F)\tau \sim 1$. The two maxima have partially coalesced for the fit to λ_2 versus T^{-1}. The very closely spaced double lines in the fit in region III (below 160 K) in Fig. 3 are a consequence of the fact that ω_F has two different values and ω_H has two different values depending on which spin species is being observed. When ^{19}F is observed [$\omega_F = 2\pi(22.50$ MHz)], $\omega_H = 2\pi(23.91$ MHz) and when ^{1}H is observed [$\omega_H = 2\pi(22.50$ MHz)], $\omega_F = 2\pi(21.17$ MHz). The greatest effect is in the terms in $\omega_H - \omega_F$ in Eqs. 18-20. The angular frequency $\omega_H - \omega_F = 2\pi(1.41$ MHz) when ^{19}F is observed at 0.5617 T and $2\pi(1.33$ MHz) when ^{1}H is observed at 0.5285 T. So, λ_1 and λ_2 versus T^{-1} each produce two sets of very closely spaced curves, much too closely spaced to be discriminated between by the experiments.

E_{NMR} and τ_∞ characterize the reorientation of the CF_3 group while $\varepsilon < 1$ suggests that there is a very small distribution of E_{NMR} values, probably because of surface effects in very small crystallites[4] or because of crystal imperfections in general. Since E_{NMR} is in the exponential of $\tau = \tau_\infty \exp(E_{NMR}/kT)$, the uncertainty in E_{NMR} leads to a very large uncertainty in τ_∞, about ± 50%. NMR relaxation experiments are not very good in determining τ_∞ accurately but the value here is in the expected range for CF_3 or CH_3 reorientation.[2, 3, 6, 8, 11, 15, 16, 101] If E_{NMR} were frozen at its

central value, the uncertainty in τ_∞ would be significantly smaller. It seems that most practitioners quote this smaller uncertainty.

We can compare the parameters y introduced in Eq. 17 and q introduced in Eq. 21 found here for **1** with the values found in **2** and **3** (Fig. 1). The parameter y characterizes the interactions between ^{19}F spins on different CF_3 groups in **1** and **3** and between ^{1}H spins in different CH_3 groups in **2**. The ordering of the experimentally determined values is $y = 0.15 \pm 0.05$ (in **1**) > $y = 0.10\ ^{+0.10}_{-0.05}$ (in $\mathbf{3}^{11}$) > $y = 0\ ^{+0.03}_{-0}$ (in $\mathbf{2}^{8}$). The parameter q characterizes the interactions between ^{1}H and ^{19}F spins in all three solids and the ordering is $q = 0.15 \pm 0.03$ (in **1**) > $q = 0.055 \pm 0.010$ (in $\mathbf{3}^{11}$) > $q = 0.020 \pm 0.005$ (in $\mathbf{2}^{8}$). The ordering is the same for both parameters and reflects the fact that the CF_3 groups in **1** have ^{1}H and ^{19}F spins closer to them than do the CH_3 groups in **2**. Compound **3** is between the two.

The relaxation curves for $q = 0$, 0.05 (close to that found for $\mathbf{3}^{11}$), 0.15 (found here for **1**), and 0.25 are shown in Fig. 6 to indicate the effect of the parameter q in Eq. 21. (For these different curves, all other adjustable parameters have been frozen at the values indicated above.) Note that all curves (including $q = 0$) closely reproduce λ_1 at high temperatures (region I) and λ_2 at low temperatures (region III). As q is increased from 0, λ_1 becomes larger at low temperatures (starting with $\lambda_1 = \lambda_2$ for $q = 0$) and λ_2 becomes larger at high temperatures (starting at $\lambda_2 = 0$ for $q = 0$).

As $T \rightarrow 0$ in region III, all four fractional equilibrium magnetizations (ϕ_{1H}, ϕ_{2H}, ϕ_{1F}, and ϕ_{2F}) $\rightarrow 0.5$. Note that the vertical positioning of the upward and downward pointing triangles in Fig. 3, when compared with those in Fig. 4, are reversed for ^{1}H but not for ^{19}F. This is why there is a subscript k on the equilibrium magnetizations in Eq. 4. Even though the two equilibrium magnetizations are the same, they are reversed, depending on which spin species is being observed.

as $T \rightarrow \infty$ in region III, $\phi_{1F}(\infty) \rightarrow 1$ for ^{19}F, $\phi_{2H}(\infty) \rightarrow 1$ for ^{1}H, $\phi_{2F}(\infty) \rightarrow 0$ for ^{19}F, and $\phi_{1H}(\infty) \rightarrow 0$ for ^{1}H. So even though the relaxation is, in principle, described by a double exponential, the magnetization associated with one of the two relaxation rates disappears as $T \rightarrow \infty$. The single surviving ^{19}F magnetization relaxes with λ_1 (region I) and the single surviving ^{1}H magnetization relaxes with λ_2 (region I). These limits are not obvious from Eq. 24 but can be

derived by inserting all the appropriate λs and Rs into Eq. 24. The caveat here is that the rates $\lambda_1 = (R_F)_S$ and $\lambda_2 = (R_H)_S$ at higher temperatures (region I) all pertain to initial rates R_S defined in Eq. 3. In this case, $R_S > R^*$ (in Eq. 2) (significantly so).[6] However, at low temperatures (region III in Figs. 3 and 4), $R_S = R^* = R$ (the usual unique relaxation rate in an exponential process) for both terms in the double exponential relaxation (Eq. 4) since $\beta = 1$ for both terms. So, the expression for the double exponential in region III is valid. That is, λ_1 is the rate characterizing the *entire* time evolution of one component of the magnetization and λ_2 is the rate characterizing the *entire* time evolution of the other component of the magnetization. To put it another way, at low temperatures λ_1 and λ_2 are *not* rates associated with the initial relaxation (of their share of the magnetization) but with the entire recovery curve (of their share of the magnetization). This is consistent with the observation that the relaxation due to CH_3 rotation in systems with no F atoms is observed to be exponential at low temperatures ($\omega_H\tau >> 1$).[2, 6, 89-95]

The straight lines drawn to guide the eye in region III in Fig. 4 show the high and low temperature trends for the ϕ_{jk} (Eqs. 5 and 24) but are, nevertheless, misleading. The expressions for the fractional equilibrium magnetizations are nonlinear in T^{-1}. The temperature region where the fractional magnetizations have been observed (Fig. 4) corresponds to a central part of the low-temperature region in the model where the functions are approximately linear. Eq. 24 indicates that the fractional magnetizations that $\rightarrow 1$ and that $\rightarrow 0$ at high temperature do so much faster above 160 K than an extrapolation of the straight lines to higher temperature in Fig. 4 would suggest and those that $\rightarrow 0.5$ at low temperature do so more slowly than an extrapolation of these straight lines to lower temperatures would suggest.

For completeness, we note that the magnetization that is *not* observed in a particular relaxation experiment starts from its equilibrium value after the perturbation (since it is not affected by the perturbation to the other spin species), then proceeds *away* from equilibrium with the larger (faster) rate λ_1 and then decays back to equilibrium with the smaller (slower) rate λ_2.

A comment is in order concerning the reorientational motion of the OCF_3 and OCH_3 groups about their respective O-C axes. Methoxy and fluoromethoxy group reorientation has been studied by both solid state NMR relaxation[2, 6, 8] and by ab initio electronic structure calculations in the solid state[2, 5, 8] in three compounds. In all three cases the methoxy or fluoromethoxy group has a very low reorientational barrier in the isolated molecule.[2, 5, 8] However, in the solid, this

reorientation is completely quenched and these groups only librate over small angles about their equilibrium positions. These librations will be at much higher vibrational frequencies than the NMR frequency. As such, the OCF_3 reorientational librations in **1**, like the OCH_3 reorientational librations in **2**, have no (direct) effect on the spin-lattice relaxation process and simply add a very fast, small-angle, time dependence of the CF_3 or CH_3 reorientation axes to the already spatial distribution of CF_3 or CH_3 reorientation axes resulting from the polycrystalline nature of the sample. (These reorientational vibrations likely have a small effect on the value of the NMR activation energy E_{NMR}.)

An additional comment is appropriate concerning the hydrogen bonding in **1** as shown in the crystal structure in Fig. 2. The molecules in the crystal arrange themselves with paired O-H . . . O and O . . . . H-O hydrogen bonds. The H atoms might very well perform a pairwise exchange but if they do so, it is not observed as a distinct motion in the ^1H relaxation rate experiments. This is probably because this motion is simply not occurring on the NMR time scale.[104] There are seven H atoms in the molecule and the OH H atom represents one-seventh of the ^1H nuclear magnetization. Signal-to-noise is good enough that additional relaxation resulting from one-seventh of the magnetization decaying at a very different rate would have been noticed in the temperature range studied. Though unlikely,[104] this exchange could be occurring at approximately the same rate that characterizes CF_3 reorientation, in which case it would not be observed as a separate motion. This OH H atom is 0.33 nm from its nearest H neighbor on the same molecule and this is close enough for spin diffusion energy conserving ^1H-^1H spin flips to contribute to the process whereby a common spin temperature is maintained.

IV. DISCUSSION

We want to gain insight into the intramolecular and intermolecular interactions in a large class of van der Waals solids composed of covalently bonded molecules having planar aromatic backbones and either a CH_3 or CF_3 group. Seven representative compounds are listed in Table II, of which **1**-**3** are shown in Fig. 1. In Sec. III, we addressed how the modulation of the ^1H-^1H, ^{19}F-^{19}F, and ^1H-^{19}F spin-spin dipolar interactions affect the NMR ^{19}F and ^1H spin-lattice relaxation. However, the interactions of interest to a larger community of scientists are (1) intramolecular bonded (covalent) interactions, (2) intramolecular and intermolecular electronic (hyperconjugation[105-107]) interactions, (3) intramolecular and intermolecular steric interactions, and

(4) intermolecular interactions somewhat arbitrarily divided into several types that the International Union of Pure and Applied Chemistry (IUPAC) bundles under the umbrella term of van der Waals interactions.[108] The segue between all these atomic and molecular interactions and the spin-spin dipolar interactions that are very well understood[27, 109-111] and of less interest to a wider community, are the solid state NMR spin-lattice relaxation experiments. The relaxation experiments are sensitive to the barrier for CH_3 or CF_3 reorientation and to the spin-spin interactions, with the important point being that the contributions (to the parameters that characterize the relaxation process) of like-spin spin-spin (^{1}H-^{1}H and ^{19}F-^{19}F) interactions and the unlike-spin spin-spin (^{1}H-^{19}F) interactions can be separated in the model, as discussed in Sec. III. When two communicating spin species are present, the NMR relaxation experiments provide more information than when only like-spin interactions (usually ^{1}H) are present.

The most important parameter that the solid state NMR relaxation experiments provide is an NMR activation energy E_{NMR}.[31-35] The relation $\tau = \tau_\infty \exp(E_{NMR}/kT)$ presented in Eq. 9 provides the mean time between reorientations for a methyl (CH_3) or fluoromethyl (CF_3) group reorienting in a three-fold or six-fold potential[2-5, 7, 8, 10, 12, 112] in a random (Poisson[113]) process. The physical origin of $\tau^{-1} = \tau_\infty^{-1} \exp(-E_{NMR}/kT)$ is the Canonical Ensemble.[113] The literature has provided a myriad of models for this relationship over the last 100 years or so but in the present case it boils down to the simplest possible two-level reorientational model. The CH_3 or CF_3 group reorientation frequency in a ground state (taken to be energy $E = 0$) is zero, assuming there is no quantum mechanical tunneling[114] which is the case here.[76-85] The reorientation frequency at the energy where the group can reorient (*defined* as E_{NMR}) is τ_∞^{-1}. The probability of being in this high energy state is given by the Canonical Ensemble Boltzmann factor[113] $\exp(-E_{NMR}/kT)$ so the mean reorientation frequency is $\tau^{-1} = \tau_\infty^{-1} \exp(-E_{NMR}/kT)$ which is the reorientation rate times the probability of being in the state where the group can reorient. This assumes that $E_{NMR} >> kT$. The smallest E_{NMR} entry in Table II is E_{NMR} = 5 kJ mol^{-1} = 602 K rotor^{-1} (the other six entries in Table II are all more than twice this) and the temperatures for the spin-lattice relaxation experiments with the compounds in Table II are all below 330 K. That this extraordinarily simple, almost naive, model works so well (i.e., fits the data in many published cases) is the basis of the great power of the solid state NMR relaxation experiments.

NMR relaxation experiments in molecular solids can determine E_{NMR} with an accuracy of approximately ± 10% or so, so long as the CH_3 or CF_3 group reorientation is the only motion on the NMR time scale in the appropriate temperature range. This is the case for many systems, including the seven compounds presented as examples in Table II. E_{NMR} can be related to the barrier V for CF_3 or CH_3 reorientation.[31-35] The lower energy for the energy difference that enters into E_{NMR} will not be zero as the naive model presented in the previous paragraph suggests, but will be the ground reorientational state which will be above the bottom of the reorientational barrier V.[31, 35] Flygare,[112] page 129, shows a reorientational energy level diagram for a CH_3 group with V = 1158 cm^{-1} = 13.8 kJ mol^{-1}. This value is typical of all but one of the entries in Table II. For the model presented in the previous paragraph, the upper energy for the energy difference that enters into E_{NMR} will be the top of the barrier, or at least near it. So one suspects that E_{NMR} might be slightly smaller than V. Indeed, detailed calculations suggest that relating E_{NMR} and V is complicated but that E_{NMR} will be between 0 and 20% smaller than V in the range of approximately 12 kJ mol^{-1}.[33, 34] This is in the middle of the range of six of the seven E_{NMR} values in Table II.

In a large class of van der Waals molecular solids comprised of covalently bonded molecules whose molecular structure in the crystal is very similar to the structure of the isolated molecule,[2-5, 7, 8, 10, 12] these barriers have contributions from both intramolecular and intermolecular interactions. For rotationally asymmetric groups like methoxy, ethyl, and isopropyl groups whose reorientational barriers are very small in many isolated molecules,[2, 5, 8, 10] these reorientational barriers, due entirely to intermolecular interactions in the solid state, are so high that reorientation is completely quenched.[2, 5, 8, 10] We are very careful to call the parameter determined in the NMR relaxation experiments the NMR activation energy E_{NMR} and not the barrier V. The latter for the case of CH_3 and CF_3 groups has been computed for several systems similar to **1**-**3** shown in Fig. 1, both in the isolated molecules and for molecules in the solid state.[2-4, 7, 8, 10, 12] Several examples of barriers in the isolated molecules are shown in Table II under the heading of V_{iso} where the subscript 'iso' means 'isolated molecule.'

Table II compares values of NMR activation energies E_{NMR} in a series of seven solids composed of molecules with similar structures. These E_{NMR} values are in very good agreement with barrier values V calculated for the appropriate rotor in the solid state[2-5, 7, 8, 10, 12] which are not given in Table II. As such, these E_{NMR} values can be taken as a stand in for the total barrier,

intermolecular + intramolecular. The entries in Table II for V_{iso}, on the other hand, are the calculated reorientational barriers for the isolated molecules and as such can be taken as a measure of the intramolecular component of the barrier. Assuming that the intramolecular potentials are not so different in the crystal than they are in the isolated molecules, the difference $E_{NMR} - V_{iso}$ can be taken as a measure of the intermolecular component of the reorientational barrier.

For the methyl group in **4**, approximately half the E_{NMR} = 5 kJ mol^{-1} is intramolecular in origin and approximately half is intermolecular in origin. This 5 kJ mol^{-1} = 601 K rotor^{-1} is, approximately, the lower limit for E_{NMR} that can be treated by the reorientational model presented in Sec. III. Indeed, this rotor will be a tunneling methyl group at lower temperatures.[114] All other entries in Table II have E_{NMR} values greater than 10 kJ mol^{-1}. In **2** (a CF_3 group with nearby ring H atoms) and **3** (a CH_3 group with nearby ring F atoms), the barriers are dominated by the intermolecular component $E_{NMR} - V_{iso}$ and in **5**, **6**, and **7** (all with a CH_3 group with nearby ring H atoms), the barriers are dominated by the intramolecular component V_{iso} . (For compounds **1**, **2**, **6**, and **7**, the methoxy/fluoromethoxy groups lie in the aromatic plane, or nearly so.) The crystal structures of all these compounds are very different and so it is difficult to generalize as to why one component should dominate in a particular compound. However, the observation that the CH_3-F and CF_3-H systems have reorientational barriers dominated by intermolecular interactions whereas the CH_3-H systems have barriers dominated by intramolecular interactions is an interesting observation. E_{NMR} = 23 kJ mol^{-1} for **1** is, by some measure, the largest E_{NMR} value in Table II but until electronic structure calculations are carried out we can't say how much of this in intramolecular in origin and how much is intermolecular in origin. The prediction, based on the preceding comments, is that it is dominated by the intermolecular component of the barrier. The current study is the first one involving a fluoromethoxy (OCF_3) group.

[1]E. Mikuli, J. Hetmanczyk, B. Grad, A. Kozak, J. W. Wasicki, P. Bilski, K. Holderna-Natkaniec, and W. Medycki, J. Chem. Phys. **142**, 064507 (2015).

[2]P. A. Beckmann, C. W. Mallory, F. B. Mallory, A. L. Rheingold, and X. Wang, ChemPhysChem **16**, 1509 (2015).

[3]X. Wang, F. B. Mallory, C. W. Mallory, H. R. Odhner, and P. A. Beckmann, J. Chem. Phys. **140**, 194304 (2014).

[4]P. A. Beckmann, K. G. Conn, C. W. Mallory, F. B. Mallory, A. L. Rheingold, L. Rotkina, and X. Wang, J. Chem. Phys. **139**, 204501 (2013).

[5]X. Wang, L. Rotkina, H. Su, and P. A. Beckmann, ChemPhysChem **13**, 2082 (2012).

[6]P. A. Beckmann and E. Schneider, J. Chem. Phys. **136**, 054508 (2012).

[7]X. Wang, P. A. Beckmann, C. W. Mallory, A. L. Rheingold, A. G. DiPasquale, P. Carroll, and F. B. Mallory, J. Org. Chem. **76**, 5170 (2011).

[8]D. P. Fahey, W. G. Dougherty Jr., W. S. Kassel, X. Wang, and P. A. Beckmann, J. Phys. Chem. A **116**, 11946 (2012).

[9]K. J. Mallikarjunaiah, R. Damle, and K. P. Ramesh, Solid State Nuc. Mag. Resonan. **34**, 180 (2008).

[10]X. Wang, A. L. Rheingold, A. G. DiPasquale, F. B. Mallory, C. W. Mallory, and P. A. Beckmann, J. Chem. Phys. **128**, 124502 (2008).

[11]P. A. Beckmann, J. Rosenberg, K. Nordstrom, C. W. Mallory, and F. B. Mallory, J. Phys. Chem. A **110**, 3947 (2006).

[12]X. Wang, F. B. Mallory, C. W. Mallory, P. A. Beckmann, A. L. Rheingold, and M. M. Francl, J. Phys. Chem. A **110**, 3954 (2006).

[13]A. J. Horsewill and I. B. I. Tomash, Solid State Nuc. Mag. Resonan. **2**, 61 (1993).

[14]G. Burbach, N. Weiden, and A. Weiss, Z. Naturforsch. **47a**, 689 (1992).

[15]F. B. Mallory, C. W. Mallory, K. G. Conn, and P. A. Beckmann, J. Phys. Chem. Sol. **51**, 129 (1990).

[16]K. G. Conn, P. A. Beckmann, C. W. Mallory, and F. B. Mallory, J. Chem. Phys. **87**, 20 (1987).

[17]A. Kozak, M. Grottel, A. E. Koziol, and Z. Pajak, J. Phys. C: Solid State Phys. **20**, 5433 (1987).

[18]W. Watton, J. C. Pratt, E. C. Reynhardt, H. E. Petch, J. Chem. Phys. **77**, 2344 (1982).

[19]J. Yamauchi and C. A. McDowell, J. Chem. Phys. **75**, 1060 (1981).

[20]J. Yamauchi and C. A. McDowell, J. Chem. Phys. **75**, 577 (1981).

[21]H. Z. Rager, Naturforsch. **36a**, 637 (1981).

[22]S. Albert and J. A. Ripmeester, J. Chem. Phys. **70**, 1352 (1979).

[23]E. C. Reynhardt, A. Watton, and H. E. Petch, J. Chem. Phys. **71**, 4421 (1979).

[24]S. Albert and H. S. Gutowsky, J. Chem. Phys. **59**, 3585 (1973).

[25]J. E. Anderson and W. P. Slichter, J. Chem. Phys. **43**, 433 (1965).

[26]R. Tilley, *Crystals and Crystal Structures* (Wiley, Chichester, UK, 2006).

[27]A. Abragam, *The Principles of Nuclear Magnetism* (Oxford Univ. Press, Oxford, 1961).

[28]L. K. Runnells, Phys. Rev. **134**, A28 (1964).

[29]R. L. Hilt and P. S. Hubbard, Phys. Rev. **134**, A392 (1964).

[30]S. Emid and R. A. Wind, Chem. Phys. Lett. **27**, 312 (1974).

[31]A. Detken, P. Focke, H. Zimmermann, U. Haeberlen, Z. Olejniczak, and Z. T. Lalowicz, Z. Naturforch. **50a**, 95 (1995).

[32]T. K. Jahnke, W. Müller-Warmuth, and M. Bennati, Solid State Nuc. Mag. Resonan. **4**, 153 (1995) .

[33]O. Edholm and C. Blomberg, Chem. Phys. **56**, 9 (1981).

[34]J. Kowaleski and T. Liljefors, Chem. Phys. Lett. **64**, 170 (1979) .

[35]E. K. van Putte, J. Mag. Resonan. **2**, 216 (1970).

[36]L. Vugmeyster, D. Ostrovosky, and A. S. Lipton, J. Phys. Chem. B **117**, 6129 (2013).

[37]L. Vugmeyster, D. Ostrovosky, K. Penland, G. L. Hoatson, and R. L. Vold, J. Phys. Chem. B **117**, 1051 (2013).

[38]J. Huang, L. Jiang, P. Ren, L. Zhang, and H. Tang, J. Phys. Chem. B **116**, 136 (2012).

[39]P. Calligari and D. Abergel, J. Phys. Chem. B, **116**, 12955 (2012).

[40]C. H. Wu, B. Bibhuti, and S. J Opella, J. Mag. Resonan. **202**, 127 (2010).

[41]R. Godoy-Ruiz, C. Guo, and V. Tugarinov, J. Am. Chem. Soc. **132**, 18340 (2010).

[42]L. Vugmeyster, D. Ostrovosky, J. J. Ford, and A. S. Lipton, J. Am. Chem. Soc. **132**, 4038 (2010).

[43]L. Vugmeyster, D. Ostrovosky, M. Moses, J. J. Ford, A. S. Lipton, G. L. Hoatson, and R. L. Vold, J. Phys. Chem. B **114**, 15779 (2010).

[44]A. J. Baldwin, T. L. Religa, D. F. Hansen, G. Bouvignies, and L. E. Kay, J. Am. Chem. Soc. **132**, 10992 (2010).

[45]D. F. Hansen, P. Vallurupalli, and L. E. Kay, J. Am. Chem. Soc. **131**, 12745 (2009).

[46]S-T. D. Hsu, L. D. Cabrita, P. Fucini, J. Chistodoulou, and C. M. Dobson, J. Am. Chem. Soc. **131**, 8366 (2009).

[47]V. Calandrini, D. Abergel, and G. R. Kneller, J. Chem. Phys. **128**, 145102 (2008).

[48]M. Krishnan, V. Kurkal-Siebert, and J. C. Smith, J. Chem. Phys. B **112**, 5522 (2008).

[49]S. Pöyry, T. Róg, M. Karttunen, and I. Vattulainen, J. Chem. Phys. B **112**, 2922 (2008).

[50]F. Voigts-Hoffman, M. Hengesbach, A. Y. Kobitski, A. van Aerschot, P. Herdewijn, G. U. Nienhaus, and M. Helm, J. Am. Chem. Soc. **129**, 13382 (2007).

[51]Y. Xue, M. S. Pavlova, Y. E. Ryabov, H. Reif, and N. R. Skrynnikov, J. Am. Chem. Soc. **129**, 6827 (2007).

[52]V. Tugarinov and L. E. Kay, J. Am. Chem. Soc. **128**, 7299 (2006).

[53]B. Reif, Y. Xue, V. Agarwal, M. S. Pavlova, M. Hologne, A. Diehl, Y. Ryabov, and N. R. Skrynnikov, J. Am. Chem. Soc. **126**, 12354 (2006).

[54]J. E. Curtis, M. Tarek, and D. J. Tobias, J. Am. Chem. Soc. **126,** 15928 (2004).

[55]M. Swart, C. F. Guerra, and M. Bickelhaupt, J. Am. Chem. Soc. **126**, 16718 (2004).

[56]R. Kohlrausch, Ann. Phys. Chem. (Poggendorff) **91**, 179 (1854). See reference 59 for a historical note concerning this paper.

[57]R. Kahlau, D. Kruk, Th. Blochowicz, V. N. Novikov, and E. A. Rossler, J. Phys. C **22**, 365101 (2010).

[58]T. C. Dotson, J. Budzien, J. D. McCoy, and D. B. Adolf, J. Chem. Phys. **130**, 024903 (2009).

[59]M. Berberan-Santos, E. N. Bodunov, and B. Valeur, Ann. Phys. (Berlin) **17**, 460 (2008).

[60]D. C. Johnston, Phys. Rev. B **74**, 184430 (2006).

[61]R. G. Palmer, D. L. Stein, E. Abrahams, and P. W. Anderson, Phys. Rev. Lett. **53**, 958 (1984).

[62]J. R. Macdonald and J. C. Philips, J. Chem. Phys. **122**, 074510 (2005).

[63]M. N. Berberan-Santos, E. N. Bodunov, and B. Valeur, Chem. Phys. **315**, 171 (2005).

[64]E. Helfand, J. Chem. Phys. **78**, 1931 (1983).

[65]C. P. Lindsey and G. D. Patterson, J. Chem. Phys. **73**, 3348 (1980).

[66]G. Williams and D. C. Watts, Trans. Far. Soc. **66**, 80 (1970).

[67]N. Bloembergen, E. M. Purcell, and R. V. Pound, Phys. Rev. **73**, 679 (1948).

[68]R. K. Wangsness and F. Bloch, Phys. Rev. **89**, 728 (1953).

[69]I. Solomon, Phys. Rev. **99**, 559 (1955).

[70]F. Bloch, Phys. Rev. **102**, 104 (1956).

[71]P. S. Hubbard, Phys. Rev. **109**, 1153 (1958). Also, see a correction in P. S. Hubbard, Phys. Rev. **111**, 1746 (1958).

[72]D. E. Woessner, J. Chem. Phys. **36**, 1 (1962) .

[73]F. Bloch, Phys. Rev. **105**, 1206 (1957).

[74]A. G. Redfield, IBM J. Res. Develop. **1**, 19 (1957); reprinted with minor revisions in Advan. Mag. Resonan. **1**, 1 (1965).

[75]K. Tomita, Prog. Theor. Phys. **19**, 541 (1958).

[76]E. O. Stejskal and H. S. Gutowsky, J. Chem. Phys. **28**, 388 (1958). See a correction in the footnote on page 973 of ref. 77.

[77]M. B. Dunn and C. A. McDowell, Molec. Phys. **24**, 969 (1972).

[78]S. Clough and A. Heidemann, J. Phys. C: Solid State Phys. **13**, 3585 (1980).

[79]S. Clough, A. Heidemann, A. J. Horsewill, J. D. Lewis, and M. N. J. Paley, J. Phys. C: Solid State Phys. **14**, L525 (1981) .

[80]S. Clough and P. J. McDonald, J. Phys. C: Solid State Phys. **15**, L1039 (1982).

[81]S. Clough, P. J. McDonald, and F. O. Zelaya, J. Phys. C: Solid State Phys. **17**, 4413 (1984).

[82]D. Cavagnat, S. Clough, and F. O. Zelaya, J. Phys. C: Solid State Phys. **18**, 6457 (1985).

[83]S. Clough, Physica **136B**, 145 (1986).

[84]M. J. Barlow, S. Clough, A. J. Horsewill, and M. A. Mohammed, Solid State Nuc. Mag. Resonan. **1**, 197 (1992).

[85]S. Clough, Solid State Nuc. Mag. Resonan. **9**, 49 (1997).

[86] J. S. Waugh and É. I. Fedin, Soviet Physics – Solid State, **4**, 1633 (1963).

[87]R. Ferrando, R. Spadacini, G. E. Tommei, and V. I. Mel'nikov, Phys. Rev. E **51**, R1645 (1995).

[88]L. Owen, in I*nternal Rotation in Molecules* (ed., W. J. Orville-Thomas, Wiley, New York, 1974, p. 157).

[89]P. A. Beckmann, Solid State Nuc. Mag. Resonan. **71**, 9 (2015).

[90]E. R. Andrew, R. Gaspar Jr., and W. Vennart, Chem. Phys. Lett. **38**, 141 (1976).

[91]K. van Putte, J. Mag. Resonan. **5**, 367 (1975).

[92]J. D. Cutnell and L. Verduin, J. Chem. Phys. **59**, 258 (1973).

[93]D. Cutnell and W. Venable, J. Chem. Phys. **60**, 3795 (1974).

[94]M. Mehring and H. Raber, J. Chem. Phys. **59**, 1116 (1973).

[95]M. F. Baud and P. S. Hubbard, Phys. Rev. **170**, 384 (1968).

[96]A. Kumar and C. S. Johnson, Jr., J. Chem. Phys. **60**, 137 (1974).

[97]N. Pislewski, J. Tritt-Goc, M. Bielejewski, A. Rachocki, T. Ratajczyk, and S. Szymanski, Solid State Nuc. Mag. Resonan. **35**, 194 (2009).

[98]Sun and A. J. Horsewill, Solid State Nuc. Mag. Resonan. **35**, 139 (2009).

[99]T. Fukunaga, N. Kumagae, and H. Ishida, Z. Naturfor. **58a**, 631 (2003).

[100]W. Davidson and R. H. Cole, J. Chem. Phys. **19**, 1484 (1951).

[101]P. A. Beckmann, L. Happersett, A. V. Herzog, and W. M. Tong, J. Chem. Phys. **95**, 828 (1991),

[102]D. Michel and V. Rossinger, J. Mag. Resonan. **28**, 235 (1977).

[103]C. Palmer, A. M. Albano, and P. A. Beckmann, Physica B **190**, 267 (1993).

[104]L. Piekara-Sady, N. Pislewski, S. Hedewy, and A. M. G. Nassar, Sol. State Comm. **67**, 1229 (1988).

[105]V. Pophristic and L. Goodman, Nature **411**, 565 (2001).

[106]I. V. Alabugin, K. M. Gilmore, and P. W. Peterson, WIREs Comp. Mol. Sci. **1**, 109 (2011).

[107]Y. Mo, WIREs Comp. Mol. Sci. **1**, 164 (2011).

[108]IUPAC, Org. Chem. Div., Pure & Applied Chem. **66**, 1077 (1994), see p 1175. Also available at (http://goldbook.iupac.org/V06597.html).

[109]C. P. Slichter, *Principles of Magnetic Resonance* (3rd ed., Springer-Verlag, Berlin, 1990).

[110]R. R. Ernst, G. Bodenhausen, and A. Wokaum, *Principles of Nuclear Magnetic Resonance in One and Two Dimensions* (Oxford Univ. Press: Oxford, 1987).

[111]R. Kimmich, *NMR Tomography, Diffusometry, Relaxometry* (Springer-Verlag, Berlin, 1997).

[112]W. H. Flygare, *Molecular Structure and Dynamics* (Prentice-Hall, Upper Saddle River, New Jersey, 1978).

[113]F. Reif, *Fundamentals of Thermal and Statistical Physics* (McGraw-Hill, New York, 1965).

[114]A. J. Horsewill, Prog. Nuc. Mag. Resonan. Spectros. **35**, 359 (1999).

Table I: Crystal data and structure refinement for 3-trifluoromethoxycinnamic acid (**1**)

CCDC deposit number	1413079
Empirical formula	C10 H7 F3 O3
Formula weight	232.16
Temperature	100(2) K
Wavelength	0.71073 Å
Crystal system	Triclinic
Space group	P-1
Unit cell dimensions	*a* = 4.7820(5) Å
	b = 6.8510(8) Å
	c = 15.4140(17) Å
	⟨ = 77.298(5)°
	® = 88.257(4)°
	© = 74.448(4)°
Volume	474.37(9) Å^3
Z	2
Density (calculated)	1.625 g/cm^3
Absorption coefficient	0.157 mm^{-1}
F(000)	236
Crystal size	0.29 x 0.14 x 0.10 mm^3
Theta range for data collection	3.69 to 26.44°
Index ranges	-5 ≤ h ≤ 4, -8 ≤ k ≤ 8, -19 ≤ l ≤19
Reflections collected	4472
Independent reflections	1860 [R(int) = 0.0307]
Completeness to theta = 26.44°	95.8 %
Absorption correction	Multi-scan
Refinement method	Full-matrix least-squares on F^2
Data / restraints / parameters	1860 / 0 / 149
Goodness-of-fit on F2	1.044
Final R indices [I>2sigma(I)]	R1 = 0.0383, wR2 = 0.0936
R indices (all data)	R1 = 0.0509, wR2 = 0.1002
Largest diff. peak and hole	0.251 and -0.256 e Å^{-3}
Recrystallization solvent	Acetone

Table II. NMR activation energies E_{NMR} and isolated-molecule calculated barriers V_{iso} for CH_3 and CF_3 reorientation in various compounds.

	compound	X in CX_3	ring atoms	E_{NMR} (kJ mol^{-1})	V_{iso}[a] (kJ mol^{-1})	E_{NMR} ref	V_{iso}[a] ref
4	3-methylphenanthrene	H	H	5 ± 1	2	16	4
3[b]	3-fluoromethylphenanthrene	F	H	12 ± 1	2	11	12
5	9-methylphenanthrene	H	H	11 ± 1	11	7	7
6	3-methoxyphenanthrene	H	H	16 ± 2	14	2	2
7	4,4'-dimethoxybiphenyl	H	H	12 ± 1	13	6	5
2[b]	4,4'-dimethoxyoctafluorobiphenyl	H	F	17 ± 1	4	8	8
1[b]	3-trifluoromethoxycinnamic acid	F	H	23 ± 2	-	this work	-

[a]The computed CH_3 or CF_3 barrier V in the isolated molecule

[b]See Fig. 1.

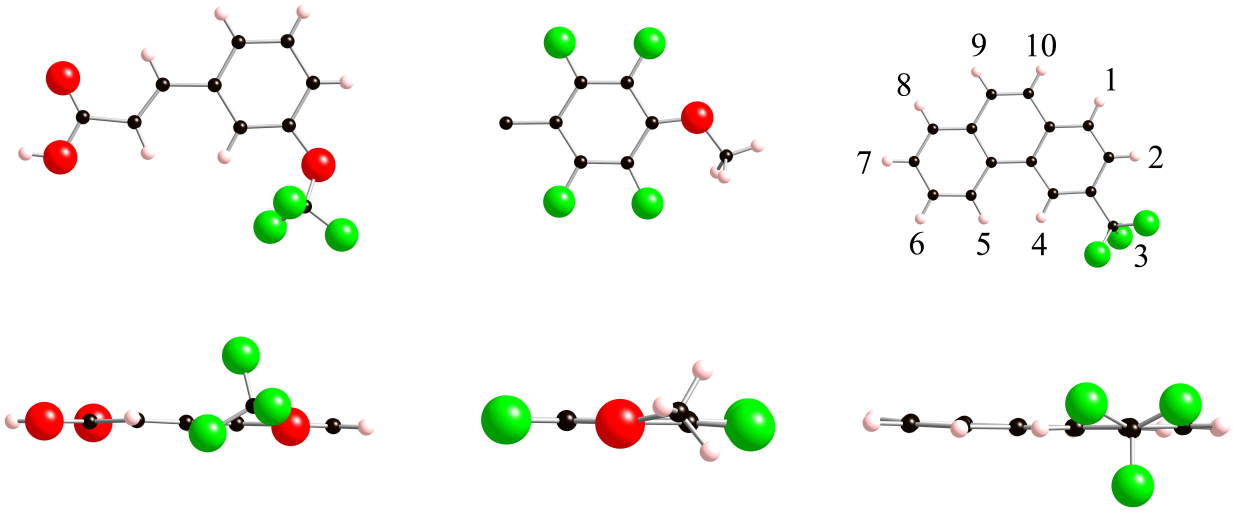

(1) **(2)** **(3)**

FIG. 1. Two views of the molecular structures in the crystal of (**1**) a molecule of 3-trifluoromethoxycinnamic acid where the asymmetric unit[26] $Z' = 1$ [this work], (**2**) half a molecule of 4,4'-dimethoxyoctafluorobiphenyl where $Z' = ½$ (CSD-WOQFAL[8]), and (**3**) a molecule of 3-fluoromethylphenanthrene where $Z' = 1$ (CSD-QCIMOD[12]). F atoms are large green spheres, O atoms are large red spheres, C atoms are small black spheres, and H atoms are small pink spheres.

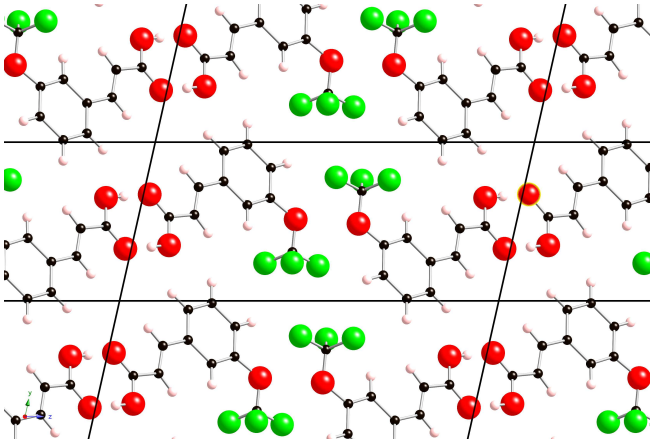

FIG. 2. The crystal structure of 3-trifluoromethoxycinnamic acid (**1**) showing the 001 plane. The lines indicate the unit cell. F atoms are large green spheres, O atoms are large red spheres, C atoms are small black spheres, and H atoms are small pink spheres.

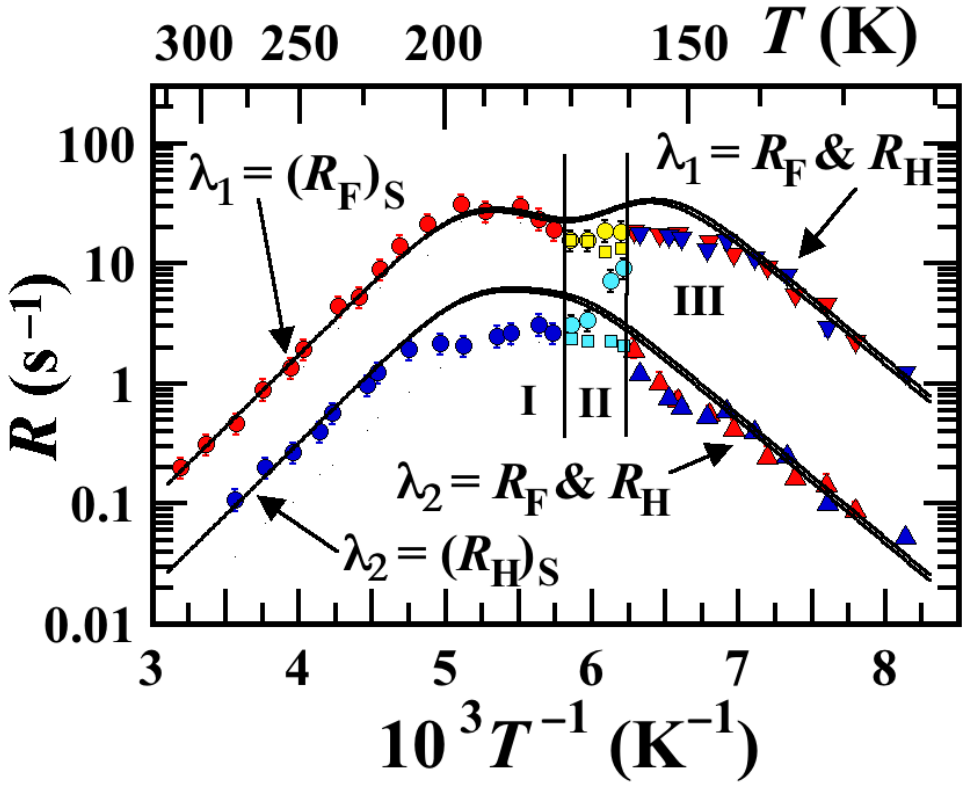

FIG. 3. The temperature dependence of the various relaxation rates in polycrystalline 3-trifluoromethoxycinnamic acid (**1**) at 22.5 MHz. At high temperatures (region I) $\lambda_1 = (R_F)_S$ as indicated (red circles) where R_S is the initial rate of the nonexponential relaxation (Eq. 3) and the subscript F refers to ^{19}F. Also in region I, the parameter $\lambda_2 = (R_H)_S$ (blue circles) where the subscript H refers to ^{1}H. At low temperatures (region III), the ^{1}H and ^{19}F magnetizations both relax via a double exponential (Eq. 4) with the same two rates, λ_1 [downward pointing triangles (red for ^{19}F and blue for ^{1}H)], and λ_2 [upward pointing triangles (red for ^{19}F and blue for ^{1}H)]. In the transition region (region II) the ^{19}F initial relaxation rates $(R_F)_S$ are indicated by yellow circles and the characteristic relaxation rates R_F^* (in Eq. 2) are indicated by yellow squares. These same two parameters for the ^{1}H relaxation in region II are indicated by cyan circles $(R_H)_S$ and cyan squares R_H^*.

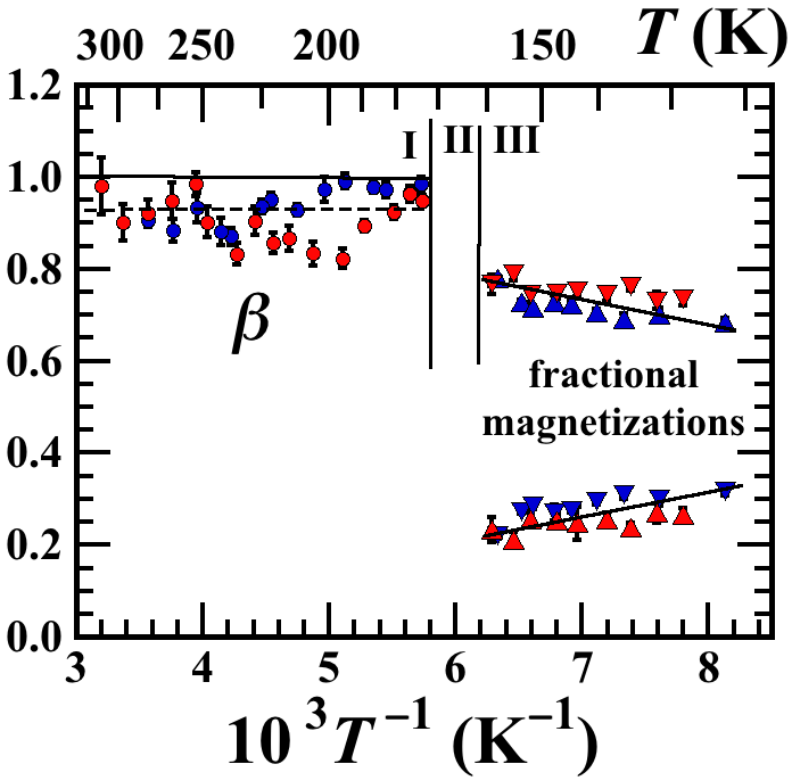

FIG. 4. The temperature dependence of various relaxation parameters for 3-trifluoromethoxycinnamic acid (**1**) at an NMR frequency of 22.5 MHz. At higher temperatures (region I) the relaxation is fitted by a stretched exponential (Eq. 2) and the plot shows β for ^{19}F (red circles) and ^{1}H (blue circles). At lower temperatures (region III) the relaxation is fitted by a double exponential (Eq. 4). The fractions of the magnetizations that relax with the rate λ_1 are ϕ_{1k} (Eqs. 5 and 24) [downward pointing triangles (red for k = F and blue for k = H) and the fractions of the magnetizations that relax with the rate λ_2 are ϕ_{2k} (Eqs. 5 and 24) [upward pointing triangles (red for k = F and blue for k = H). The two straight lines, which add to unity, are guides for the eye.

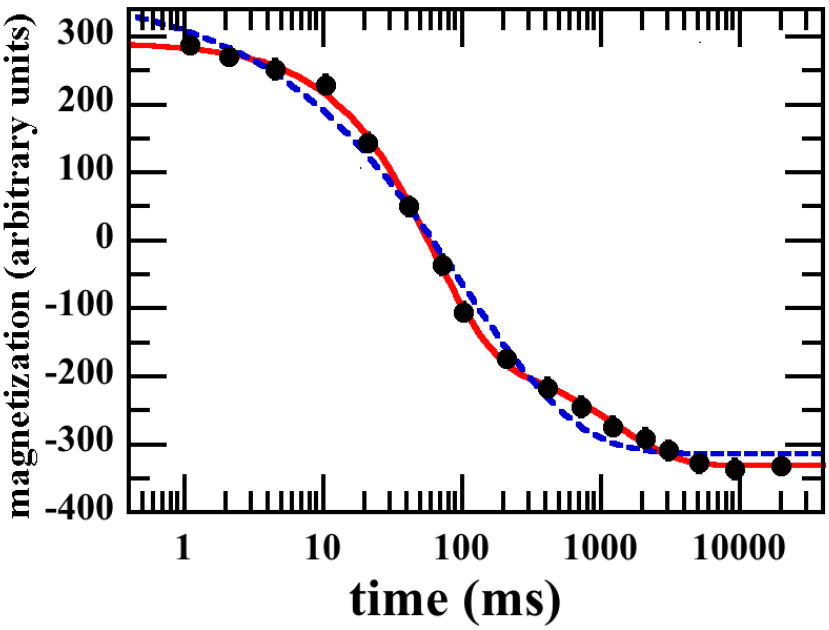

FIG. 5. A ^{19}F magnetization recovery curve in polycrystalline 3-trifluoromethoxycinnamic acid (**1**) at 22.5 MHz and at 152 K (region III in Figs. 3 and 4). The recovery time between the perturbation π-pulse and the observing π/2 pulse is plotted on a logarithmic scale for visual clarity. The (good) five-parameter fit to the double exponential in Eq. 4 (solid red line) gives the two relaxation rates λ_1 and λ_2 shown in Fig. 3 and the corresponding fractional equilibrium magnetizations ϕ_{1F} and ϕ_{2F} shown in Fig. 4. The smaller (slower) rate was $\lambda_2 = 0.75 \pm 0.11$ s^{-1} for this particular experiment and t_w [the time between the observing π/2 pulse and the (next) perturbation π pulse] was $t_w = 15$ s which is greater than 10 λ_2^{-1}. For comparison, the (bad) four parameter fit to the stretched exponential (Eq. 2) is shown by the blue dashed line.

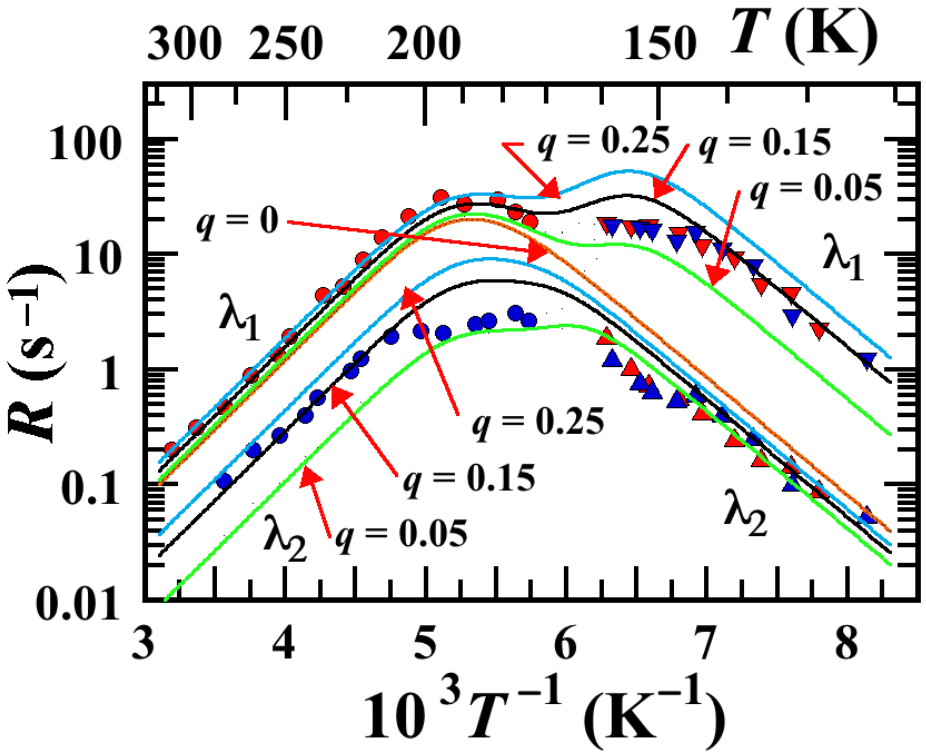

FIG 6. The effect of ^{1}H-^{19}F spin-spin interactions on the ^{19}F and ^{1}H spin-lattice relaxation rates in polycrystalline 3-trifluoromethoxycinnamic acid (**1**) at 22.5 MHz. The relaxation rate data is described in the caption to Fig. 3. The phenomenological scalar parameter q defined in Eq. 21 (with values as indicated) describes the cumulative effects of ^{1}H-^{19}F spin-spin interactions as a fraction of the intraCF_3 ^{19}F-^{19}F spin-spin interactions. The ^{1}H-^{19}F spin-spin interactions are turned off for $q = 0$ and there is a single R_F as indicated by the single line. In this case $R_H = 0$. As q is increased from 0, a second set of curves appear. The two lines labeled $q = 0.15$ corresponds to the final fit value for **1** and are the same as those in Fig. 3.